SciEn

Proceedings of 8th International Conference on Mechanical, Industrial and Energy Engineering 2024
02-04 January, 2025, Khulna, BANGLADESH

SciEn Conference Series: Engineering Vol. 3, 2025, pp 213-221 https://doi.org/10.38032/scse.2025.3.57

Advanced Numerical Study on Natural Convection Heat Transfer in an Inverted T-Shaped Cavity Filled with Copper Nanofluid

Gopal Sen[1], *Md Saifur Rahman*[1,*], *Khairun Nasrin Rimi*[2], *Md Shahjahan Durjoy*[3]

[1]Department of Mechanical Engineering, Chittagong University of Engineering and Technology, Chattogram 4349, Bangladesh
[2]Department of Mechanical Engineering, Bangladesh University of Engineering & Technology, Dhaka-1000, Bangladesh
[3]Department of Mechanical and Production Engineering, Ahsanullah University of Science & Technology, Dhaka-1208, Bangladesh

ABSTRACT

The aim of this analysis is to report on the behavior of Copper-Air (Cu-Air) nanofluid natural convection heat transfer within an inverted T-shaped enclosure having differentially heated sidewalls. The left margins of the enclosed cavity have been treated as a heated wall and hence they are kept at a constant temperature. The right edges, though not as hot as the heated wall, are also maintained at a constant temperature. The horizontal walls of the cavity were assumed to be adiabatic. Numerical investigation of the evaluation was made using ANSYS Fluent. The effects of different important parameters, such as the shape of the enclosure, Rayleigh number, and volume fraction of nanoparticles on heat transfer characteristics inside an inverted T-shaped enclosure, have been studied. In the numerical analysis, a set of DNSs has been done for different Rayleigh numbers in the 10^3 to 10^6 range, with a volume fraction of the particles in the range $0 \leq \varphi \leq 0.1$, and for several aspect ratios of the inverted T-shape. These results of this CFD analysis, therefore, depict an extraordinary increase in the volume-averaged heat transfer coefficient with increasing volume fraction of Cu particles in air. Also, it was noticed that the volume-averaged Nusselt number increases as the Rayleigh number increases, though there is a slight fall at higher volume fractions of nanoparticles due to higher conduction heat transfer. For Rayleigh numbers $\geq 10^4$, both the average Nusselt number and average heat transfer coefficient decreases up to a certain shape of the cavity aspect ratio. Beyond that, the values of both parameters increase. In the case of Rayleigh number = 10^3, the value is decreased for both with the increase in the cavity aspect ratio.

Keywords: Natural convection, Inverted T shape, Cu nanoparticle, CFD, Nusselt number.

1. Introduction

In recent years, convection flow in complex geometries has received growing attention. This is due to the increased use of natural convection in various engineering applications such as solar heating systems, power electronic devices, cooling of electronic equipment, cooling of a chamber containing heated electronic chips, design of chemical reactors, and cooling of nuclear reactor containment structures in the case of power failure. Natural convection heat transfer is encountered in many industrial processes and in most applications, including heat exchangers, hot air allowing with solar elements enclosures like photovoltaic-thermal solar systems, electronic packages and chip cooling, and building and chimney heating. The superior thermophysical properties and the heat transfer capability of nanofluids can be used as an important fluid in cooling devices. It has been proved that nanofluid exhibits much higher thermal conductivity than conventional fluids with only a small volume fraction of the nanoparticles. Thus, it can be considered a good fluid medium for heat transfer, which can offer a much larger heat transfer rate, either by natural convection or by forced convection.

Choi and Eastman [1] revolutionized heat transmission in fluid with their invention of nanofluids in 1995. Nanofluids use particle sizes ranging from 1 to 100 nm. Particles can be composed of metals like copper, silver, or oxides like aluminum, copper, and diamond oxide, as well as carbon nanotubes [2]. Numerous numerical studies on the thermal properties of nanofluids have been conducted [3-10], but further research is necessary. An experimental investigation of the convection phenomena in a rectangular cavity exposed to radiation thought to be a source of thermal excitation was conducted by Karatas et al. [11]. In the same context, Ismael et al. [12] conducted a numerical study on convection in a ventilated cavity. As a result, several numerical techniques have been used to address the convection issue in cavities. Haouat et al. [13] have employed the Lattice Boltzmann Method (LBM) to examine the same issue. Wang et al. [14] have chosen to analyze convection in a hollow with a porous material using the Chebyshev spectral technique. Esfe et al. [15] used a statistical approach to analyze the thermal conductivity of CNTs-Al2O3/water nanofluid, finding that the thermal conductivity of the nanofluid increases with both temperature and solid volume percentage. Khanafer et al. [16] studied natural convection in a two-dimensional container with nanofluids. The researchers compared various nanofluid models based on their physical features. Kaviny [17] investigated the impact of a semi-cylinder at the bottom of an enclosure on heat transfer rates. The study found that having a protuberance reduces heat transmission rates in the enclosure's lower section. Freidoonimehr et al. [18] investigated the transient MHD natural convection of a

*Corresponding Author Email Address: mdsaifur.rahman.me@gmail.com

nanofluid on a vertical surface. Nanofluids containing Al2O3 and Cu nanoparticles had the lowest and highest skin friction coefficients, respectively. Furthermore, distributed Cu and TiO2 nanoparticles in a base fluid exhibit the the largest and lowest heat transfer rates. Mohebbi and Rashidi [19] investigated the natural convection of a nanofluid in an L-shaped container and they found that heat transfer and flow field are significantly affected by heat source position. Placing a heat source in the cavity's lower and left walls results in a significant heat transfer rate, regardless of aspect ratio. Izadi et al. [9] investigated the impact of source-sink arrangements on a laminar mixed nanofluid flow with Al2O3 nanoparticles in a cavity. The optimal configuration had a Nusselt number of 15 or higher. Mehrizi et al. [20] observed that increasing the volume percentage of nanoparticles boosted the heat convection rate utilizing the LBM analysis. Furthermore, Sebdani et al. [21] explored the mixed convection of an Al2O3/water nanofluid with temperature-dependent thermal conductivity. Mohebbi et al. [22] recently completed a numerical simulation of forced convection throughout an extended-surface channel employing three different nanofluids. They concluded that a specific arrangement of extended surfaces could improve heat transfer rates.

2. Problem Statement

Fig. 1 illustrates the configuration of the inverted-T cavity. The upper boundary is denoted as x, and the lower boundary is defined as L, with L set at 0.1 m. The study analyzes several ratios of x/L, denoted by the symbol χ. Significantly, the condition x = y is preserved across all examined cavity geometries.

Initially, the investigation focused on free convective heat transfer properties using air as the working medium inside the cavity. Subsequently, nanoparticles were incrementally introduced into the medium to analyze their impact. Air is used as the base fluid of the nanofluid, which contains Cu nanoparticles. In this study, Cu nanoparticles were mixed with air at 1-10% volume fraction, with an average of 2 nm in diameter. Average heat transfer coefficient and average Nusselt number values were determined in a wide series of Rayleigh numbers, between 10^3 and 10^6.

In this direct simulation, the flow was considered to be steady, incompressible, and two-dimensional (2D). Furthermore, the Boussinesq approximation was employed throughout all of these DNS simulations. The current numerical study aims to investigate the natural convection heat transfer characteristics of Cu-air nanofluid in an inverted T-shaped cavity. The analysis examines different Rayleigh numbers, particle volume fractions, and geometric characteristics.

2.1 Boundary Conditions

The temperature of the heated wall is maintained at a constant value of 310 K, while the cooled wall is kept at 300 K. The flow within the cavity is assumed to be laminar. The upper and lower walls of the cavity, denoted as x and L in Fig. 1, are treated as thermally insulated. Additionally, it is presumed that the base fluid (air) and the nanoscale particles in the mixture are in thermal equilibrium, with a no-slip condition applied between them. Also, the variation of thermo-physical properties of the nanofluid are constant except for density and is approximated by the Boussinesq model.

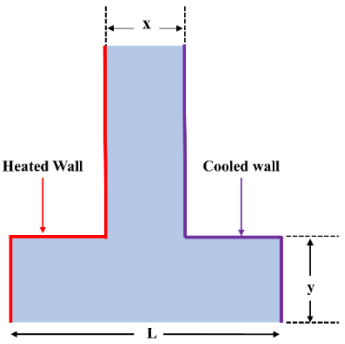

Fig.1 Boundary conditions of the inverted T shaped enclosure

3. Mathematical Modeling Details

The governing equations employed for this study, incorporating the Boussinesq approximation, include the continuity equation, momentum equations, and energy equation. These equations describe laminar and steady-state natural convection heat transfer within the two-dimensional enclosure and are expressed in their dimensional forms as follows:

Continuity Equation for mixture model:

$$\frac{\partial}{\partial t}(\rho_m) + \nabla.(\rho_m \overrightarrow{v_m}) = 0 \quad (1)$$

where $\overrightarrow{v_m}$ represents mass-averaged velocity and ρ_m denotes the density of mixture.

Momentum Equation for mixture model:

$$\frac{\partial}{\partial t}(\rho_m \overrightarrow{v_m}) + \nabla.(\rho_m \overrightarrow{v_m}\,\overrightarrow{v_m}) = -\nabla p + \nabla.[\mu_m(\nabla.\overrightarrow{v_m} + \nabla.\vec{v}_m^{T})] + \rho_m \vec{g} + \vec{F} + \nabla.\left(\sum_{k=1}^{n} \alpha_k \rho_k \vec{v}_{dr,k}\vec{v}_{dr,k}\right) \quad (2)$$

where *n* denotes number of phases. $\vec{F}$ is the body force and μ_m equals to the viscosity of the mixture. $\vec{v}_{dr,k}$ is denoted as the drift velocity for the secondary phase, *k*.

Energy Equation for mixture model:

$$\frac{\partial}{\partial t}\sum_{k=1}^{n}(\alpha_k \rho_k E_k) + \nabla.\sum_{k=1}^{n}(\alpha_k \vec{v}_k(\rho_k E_k + p)) = \nabla.(k_{eff}\nabla T) + S_E \quad (3)$$

where k_{eff} is the effective conductivity $(\sum \alpha_k(k_k + k_t))$, where k_t represents the turbulent thermal conductivity defined based on the selected turbulence model. The first term on the right-hand side of Equation (6) corresponds to energy transfer via conduction. S_E accounts for any other volumetric heat sources present in the system.

The nanofluid's effective density (ρ_{nf}) and heat capacitance $(\rho c_p)_{nf}$ are defined as follows [9]:

$$\rho_{nf} = (1-\varphi)\rho_f + \rho_s \varphi \quad (4)$$

$$(\rho C_p)_{nf} = (\rho C_p)_f (1-\varphi) + (\rho C_p)_s \varphi \quad (5)$$

Here φ represents the solid volume fraction of nanoparticles in the mixture. Thermal diffusivity of the nanofluids is represented by α_{nf},

$$\alpha_{nf} = \frac{k_{nf}}{(\rho c_p)_{nf}} \quad (6)$$

Also, the thermal expansion coefficient of the nanofluids has been calculated using the following equation,

$$\beta_{nf} = \beta_f (1-\varphi) + \beta_s \varphi \quad (7)$$

The dynamic viscosity equation for nanofluids, as presented by Brinkman [10] is as follows:

$$\mu_{nf} = \frac{\mu_f}{(1-\varphi)^{2.5}} \quad (8)$$

The effective thermal conductivity of nanofluid can be estimated by the Maxwell–Garnetts [11] model as following:

$$\frac{k_{nf}}{k_f} = \frac{k_s + 2k_f - 2\varphi(k_s - k_f)}{k_s + 2k_f + 2\varphi(k_s - k_f)} \quad (9)$$

The application of equation (9) is limited to spherical nanoparticles, making it inapplicable to nanoparticles of other shapes of nanoparticles.

The Nusselt number and Rayleigh number are expressed as follows:

$$Nu = \frac{hL}{k}$$
$$Ra = \frac{g\beta\Delta T x^3}{\nu\alpha} \quad (10)$$

The thermo-physical properties of the base fluid, air and Copper nano-particle are presented in table 1 below:

Table 1 Thermophysical properties of Air [12] and nano-particle [25]

Property		Air	Cu
ρ	(kg/m^3)	1	8920
C_p	(J/kgK)	1006.43	385
K	(W/mK)	0.0242	398
β	(1/K)	3.2*10^{-9}	1.6*10^{-5}

4. Results and Discussion

4.1 Grid Independence Test

The solutions derived from different mesh sizes have been examined to confirm grid independence. A grid independence test has been conducted for an enclosure with an x/L ratio of 0.5. The cavity is assumed to be filled with air and 1% Cu nanofluid mixture. The test was conducted for Ra=10^5, with the average Nusselt number documented for each mesh configuration. The meshes has been generated using the all-triangular method. From the graph, it is evident that the average Nusselt number shows the minimal variation for mesh sizes beyond 30,000 elements.

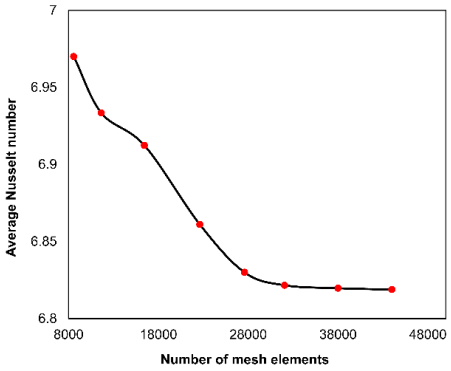

Fig. 2 Variation of the average Nusselt number with the mesh elements

4.2 Model Validation

The model has been validated by juxtaposing its results with those documented in two prior investigations, as depicted in Fig. 3. A suitable case for validation entails natural convection in air within a square cavity, where two vertical walls are held at disparate temperatures, while the upper and lower surfaces are adiabatic. The average Nusselt number for the air-filled square cavity was determined for four different Rayleigh numbers. These results were then compared with data available in the literature to ensure the model's accuracy. Present work shows an analytical consistency with the works of N.C. Markatos [23] and Vahl Davis [24], the percentage deviations in the Nusselt number being within the range 0.3-4.7%, which reinforces the validity of the analytical approach used in this work.

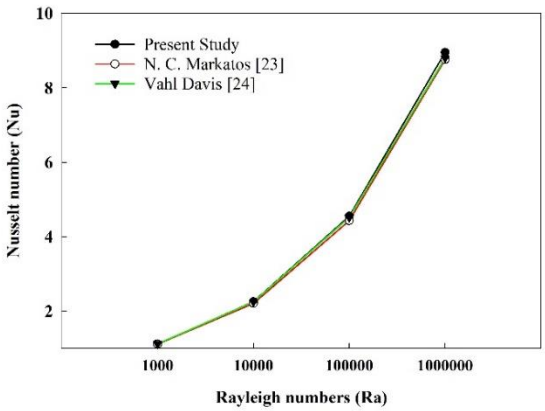

Fig. 3: Comparison of average Nusselt numbers for an air-filled square enclosure from this study and previous works at various Rayleigh numbers.

Consequently, the average Nusselt number values obtained in the present study closely align with those reported in the literature.

4.3 Effects of Nanoparticle Volume Fraction on Average Heat Transfer

The effects of nanoparticles on stream functions and temperature distribution are illustrated in Fig. 4 to 19 for χ= 0.4, 0.6, and 0.8; along with nanoparticles for Ra= 10^3, 10^4, 10^5 and 10^6. It is also observed that with an increase in the

particle volume fraction, the velocity components rise slowly, thereby speeding up the energy transport in the nanofluid inside the cavity.

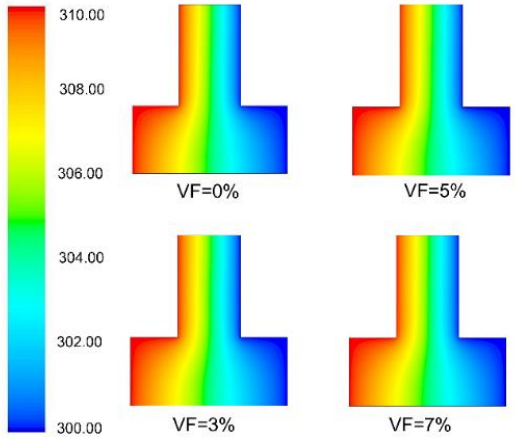

Fig.4 Contours of Static temperature with and without Nanoparticle (For χ= 0.4 and Ra=1000)

The actual values of the stream function indicate that strength of the flow increases as the nanofluid volume fraction in air gradually rises. Consequently, the streamlines become more regular in shape with higher volume fractions. The maximum stream function values also increase with the rising volume fraction, leading to more uniform streamline contours at higher volume fractions. This behavior is attributed to the improved equivalent thermal conductivity. At lower volume fractions, the temperature change inside the fluid is somewhat less pronounced than that found at higher volume fractions. The alteration in temperature distribution is more pronounced for high volume fractions than for low volume fractions.

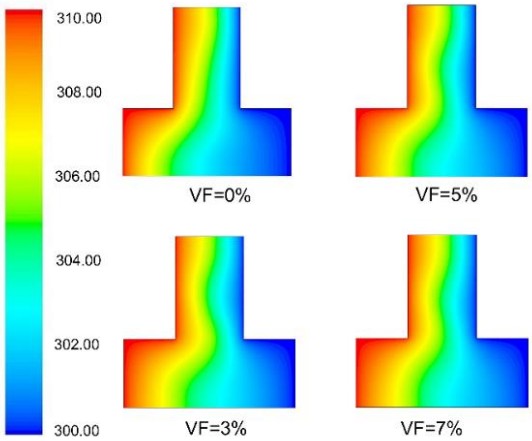

Fig.5 Static temperature contours with and without Nanoparticle (For χ= 0.4 and Ra=10000)

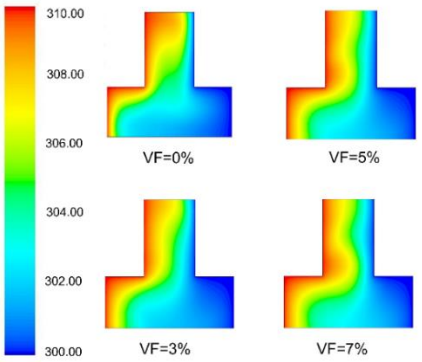

Fig.6 Static temperature contours with and without Nanoparticle (For χ= 0.4 and Ra=100000)

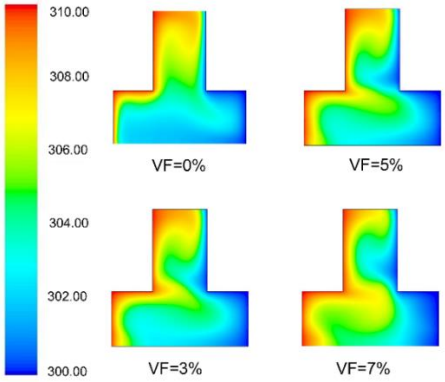

Fig.7 Static temperature contours with and without Nanoparticle (For χ= 0.4 and Ra=1000000)

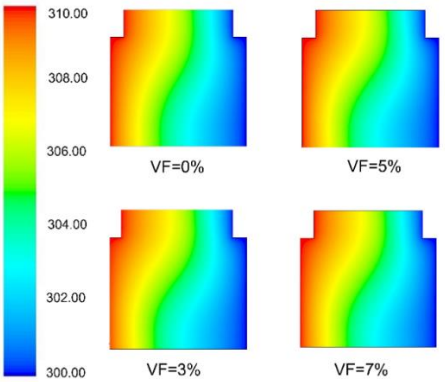

Fig.8 Static temperature contours with and without Nanoparticle (For χ= 0.8 and Ra=1000)

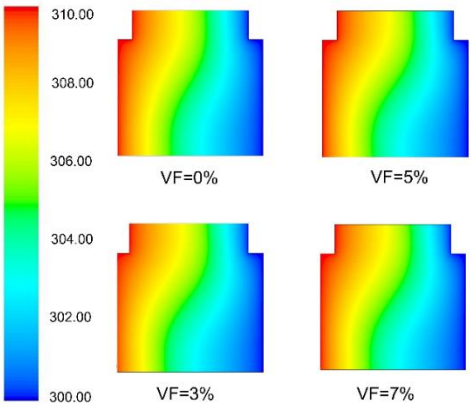

Fig.9 Static temperature contours with and without Nanoparticle (For χ= 0.8 and Ra=10000)

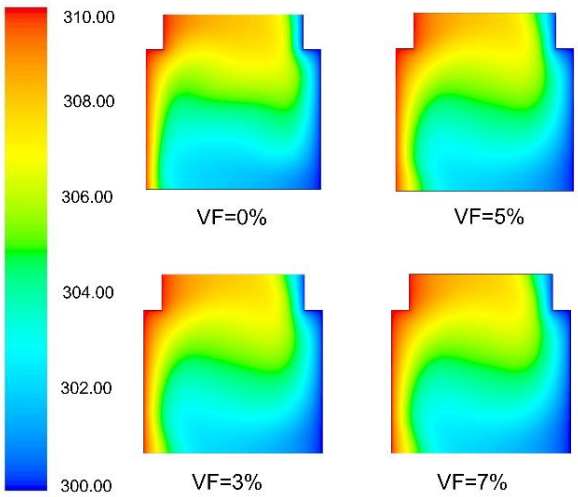

Fig.10 Static temperature contours with and without Nanoparticle (For χ= 0.8 and Ra=100000)

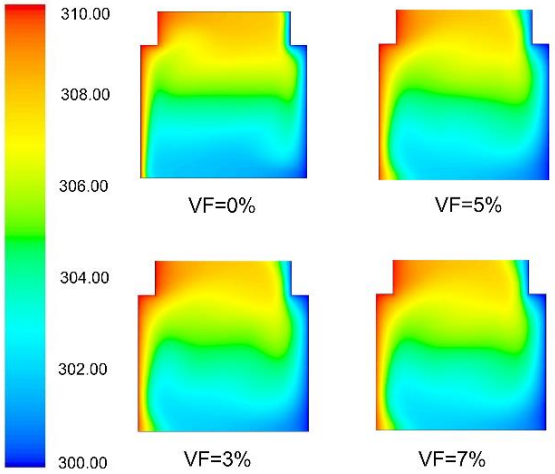

Fig.11 Static temperature contours with and without Nanoparticle (For χ= 0.8 and Ra=1000000)

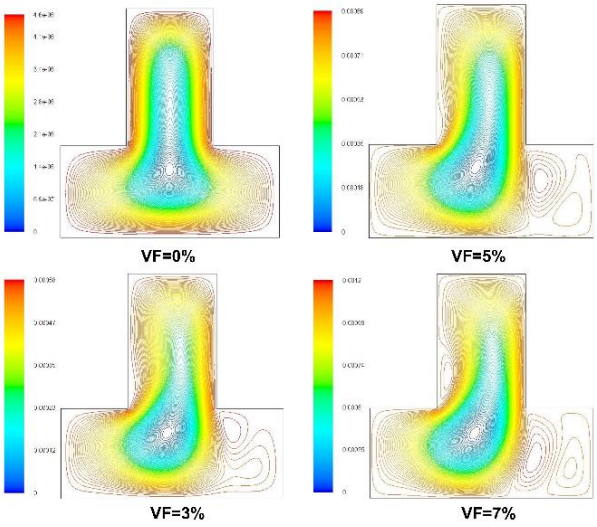

Fig.12 Stream function contours with and without Nanoparticle (For χ= 0.4 and Ra=1000)

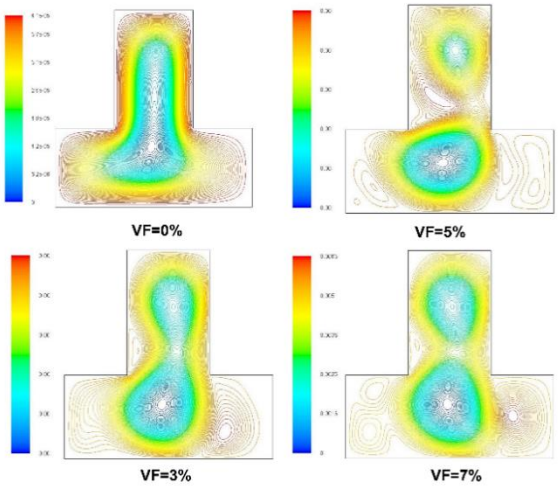

Fig.13 Stream function contours with and without Nanoparticle (For χ= 0.4 and Ra=10000)

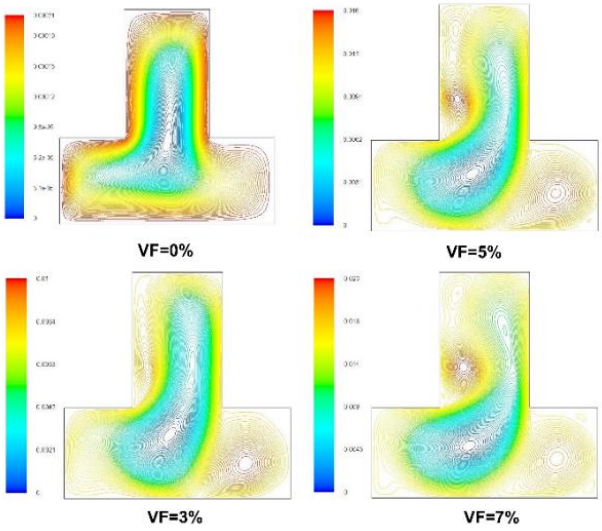

Fig.14 Stream function contours with and without Nanoparticle (For χ= 0.4 and Ra=100000)

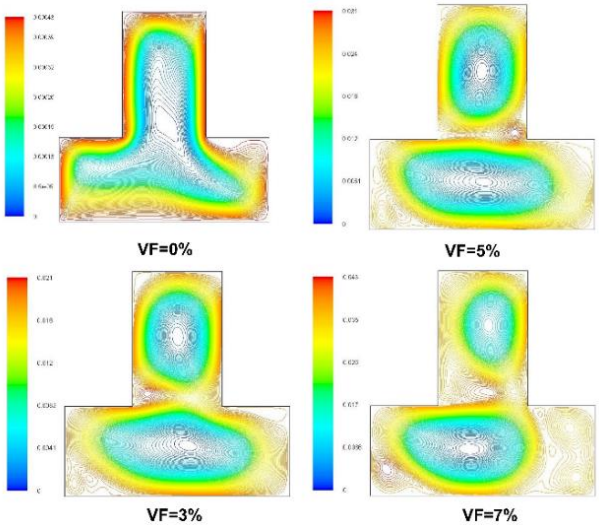

Fig.15 Stream function contours with and without Nanoparticle (For χ= 0.4 and Ra=1000000)

A higher rate of thermal conductivity in nanofluids can be achieved by increasing thermal diffusivity. Elevated thermal diffusivity minimizes temperature gradients within the fluid, leading to an increase in the thickness of the thermal boundary layer. This growth in boundary layer thickness

results in a reduced Nusselt number, indicating a lower rate of convective heat transfer relative to conduction.

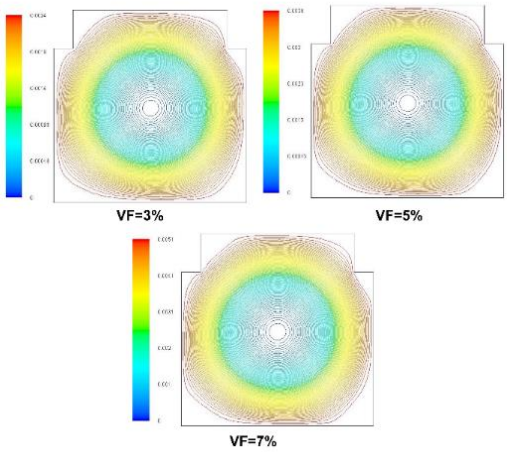

Fig.16 Stream function contours with and without Nanoparticle (For χ= 0.8 and Ra=1000)

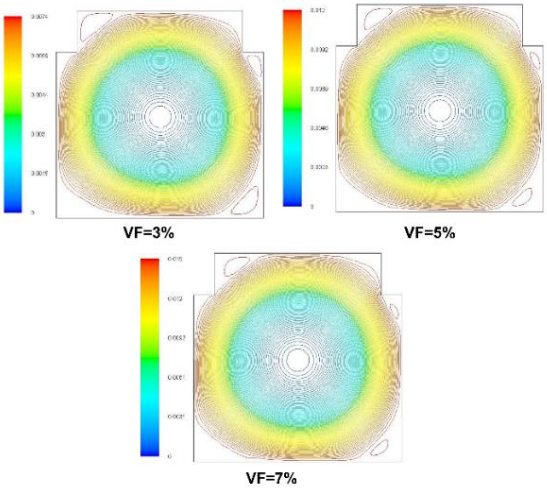

Fig.17 Stream function contours with and without Nanoparticle (For χ= 0.9 and Ra=10000)

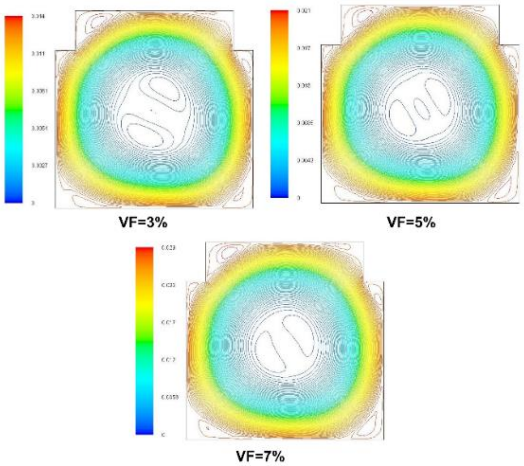

Fig.18 Stream function contours with and without Nanoparticle (For χ= 0.9 and Ra=100000)

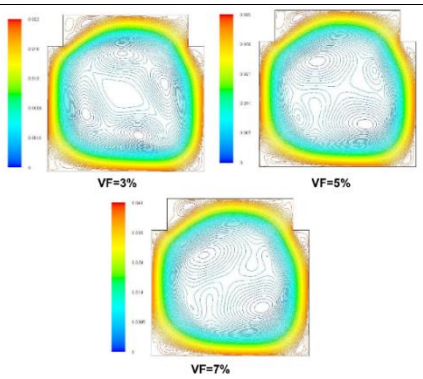

Fig. 19 Stream function contours with and without Nanoparticle (For χ= 0.9 and Ra=1000000)

With an increase in the Rayleigh number, the flow becomes more vigorous, as reflected in the rise of the maximum stream function values. This behavior is primarily driven by the enhanced buoyancy forces associated with higher Rayleigh numbers. The impact of the Rayleigh number on thermal performance parameters, such as the average Nusselt number and the average heat transfer coefficient, is evident in the figures. These parameters increase progressively with higher Rayleigh numbers, highlighting improved convective heat transfer in all enclosure geometries examined.

The contours above clearly illustrate the variation in temperature and stream function for different x/L ratios of the cavity (χ). As the value of χ increases, significant changes in the contours are observed. Analysis of the contours indicates that both temperature distribution and stream function reach to prominently maximum as χ approaches unity.

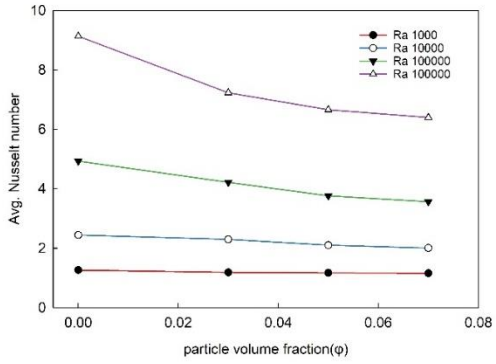

(a)

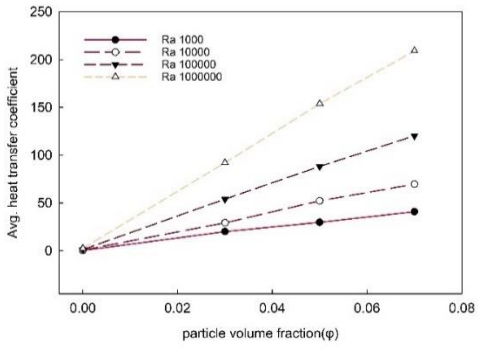

(b)

Fig.20 Variation of (a) average Nusselt number and (b) average convective heat transfer coefficient with volume fraction for various Rayleigh numbers. (for χ= 0.4)

From the fig. 20 its seen that increment of the volume fraction of nanoparticles escalates the performance in heat

transfer. For instance, the heat transfer coefficient surges from 20.026 at 10^3 to 92.1233 at 10^6 when the volume fraction reaches 3%. Again, it rises from 29.771 at 10^3 to 153.8 at 10^6 at 5%. Similarly, at 7% volume fractions, the heat transfer coefficient peaks from 40.883 at 10^3 up to 209.111 at 10^6.

Contrarily, the average Nusselt number increases with a different trend. It starts at 1.258 for a volume fraction of 0.000 and decreases to 1.182 at 3% for 10^3. It further drops to 1.163 at 5%, 1.1527 at 7% before increasing to 9.134 at 10^6 for the same volume fractions. This reflects that while the heat transfer coefficients may have improved, the average Nusselt number decreases with the rise in nanoparticle volume fraction in the basic dilutions. This shows that the relation of volume fraction with heat transfer enhancement is nonlinear.

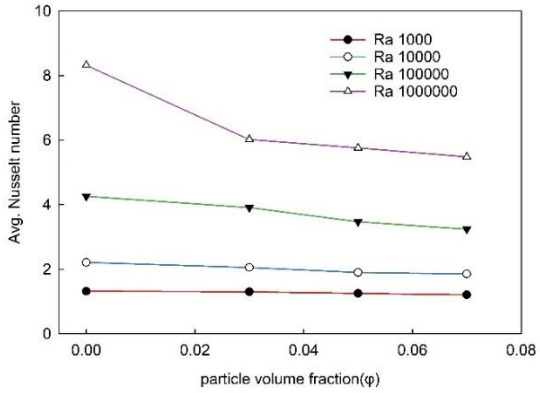

(a)

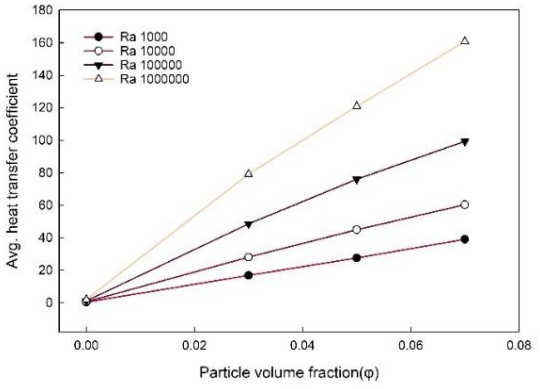

(b)

Fig.21 Variation of (a) average Nusselt number and (b) convective heat transfer coefficient with volume fraction at different Rayleigh numbers. (for χ= 0.6)

It is interpreted from the figure 21 that the average Nusselt number decreases from 1.320 at 0% to 1.208 at 7%, while the heat transfer coefficients significantly increase with the rise in the nanoparticle volume fraction (VF), going up from 0.330 to 160.727. Surprisingly, the coefficients achieve 79.105 at 3%, while reaching a maximum at 160.727 at 7%, stating that the increment is nonlinear. It appears that the volume fraction, where maximum heat transfer is taking place, should lie between 3% and 7%, stating the possibility of effectively carrying out thermal management optimization.

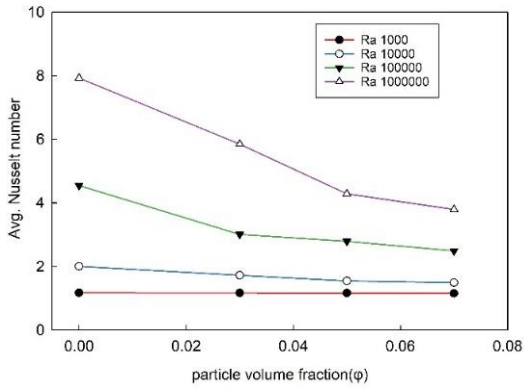

(a)

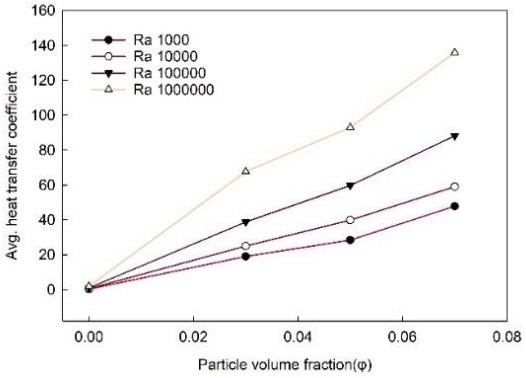

(b)

Fig.22 Variation of (a) average Nusselt number and (b) convective heat transfer coefficient with volume fraction at different Rayleigh numbers. (for χ= 0.8)

The figure 22 indicates that the average Nusselt number decreases from 1.172 at a volume fraction of 0% to 1.1535 at 7%, while the heat transfer coefficients increase significantly, starting at 0.3538 and reaching 135.87 at a volume fraction of 7%. This depicts a nonlinear relationship, and the most probable value of the volume fraction for which the enhancement in the heat transfer is greatest falls between 3% and 7%, hence giving a good avenue for greater thermal management.

4.4 Effect of Rayleigh Number on Heat Transfer

Figures 23–26 depict the contours of static temperature and stream functions. As the Rayleigh number increases, significant changes are observed in the contours. For lower Rayleigh numbers, the variation in contours is minimal. However, as the Rayleigh number rises, the temperature distribution shows notable changes. Similarly, for the stream function, the maximum magnitude increases with higher Rayleigh numbers, driven by buoyancy effects.

Figures 20–22 illustrate the effect of the Rayleigh number on both the average Nusselt number and the average heat transfer coefficient. Both parameters show a consistent increase with the rise in Rayleigh number across all enclosure shapes, indicating enhanced convective heat transfer.

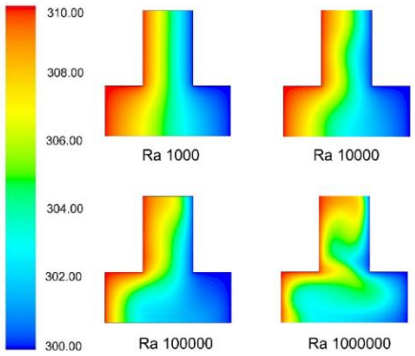

Fig.23 Static temperature contours for different Rayleigh number (for φ = 0.1 and χ =0.3)

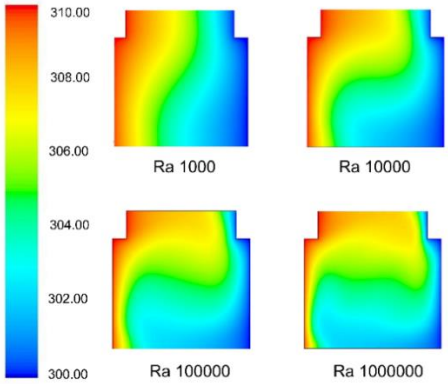

Fig.24 Contours of Static temperature for different Rayleigh number (for φ = 0.1 and χ =0.9)

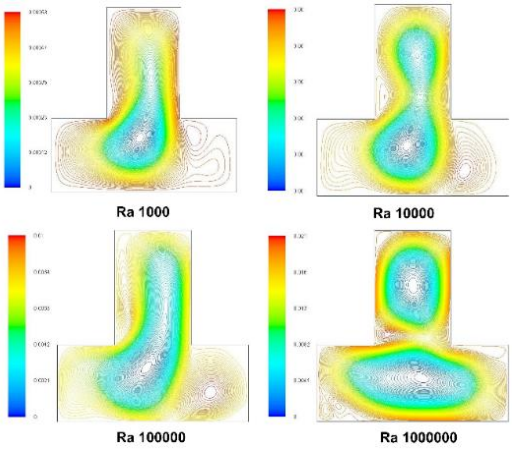

Fig.25 Contours of Streamlines for different Rayleigh number (for φ = 0.1 and χ =0.4)

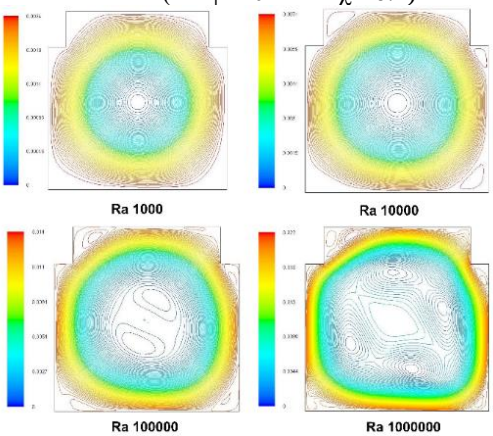

Fig.26 Contours of Streamlines for different Rayleigh number (for φ = 0.1 and χ =0.8)

5. Conclusion

The analysis shows that the volume fraction of the nanoparticles, Rayleigh number, and x/L ratio are some of the most important parameters controlling the heat transfer performance in Cu-air nanofluid.

1. There is an astonishing increase in average heat transfer coefficients that increase from 0.272 at 0% volume fraction to 209.11 at 7% for Ra=10^6.
2. The average Nusselt number decreases from 1.258 at 0% to 1.1527 at 7%: this describes an improvement in the heat transfer while the efficiency, as measured by the Nusselt number, diminishes.
3. The Nusselt number is reduced somewhat at the lowest Rayleigh numbers, Ra = 10^3 and 10^4, but at higher values, Ra = 10^5 and 10^6, the reduction becomes profound, with values falling from 4.929 at Ra = 10^5 to 4.550 at Ra = 10^6 for a volume fraction of 5%.
4. The Nusselt number and the average heat transfer coefficient decrease as x/L increases up to 0.6, beyond which they start rising for values of Ra≥ 10^4, while for Ra = 10^3, they continue decreasing.

In general, the average heat transfer coefficient and Nusselt number increased as the Rayleigh number was increased, indicating a positive response of thermal performance to increased intensity of convection. The results of this work thus tend to give an edge to nanofluids over conventional heat transfer fluids and open the possibility for making optimizations of thermal management systems via adequate selections of volume fractions of nanoparticles. Future research could be done at much higher nanoparticle concentrations and in various geometries of the cavity so as to learn more about nanofluid behavior in thermal use.

References

[1] Choi and Eastman, Eds., *Enhancing thermal conductivity of fluids with nanoparticles*. [Online]. Available: https://www.osti.gov/biblio/19652

[2] Maxwell, "A Treatise on Electricity and Magnetism,"[Online]. Available: https://www.aproged.pt/biblioteca/MaxwellI.pdf

[3] M. Izadi, A. Behzadmehr, and D. Jalali-Vahida, "Numerical study of developing laminar forced convection of a nanofluid in an annulus," *International Journal of Thermal Sciences*, vol. 48, no. 11, pp. 2119–2129, May 2009.

[4] F. Garoosi, L. Jahanshaloo, M. M. Rashidi, A. Badakhsh, and M. E. Ali, "Numerical simulation of natural convection of the nanofluid in heat exchangers using a Buongiorno model," *Applied Mathematics and Computation*, vol. 254, pp. 183–203, Jan. 2015.

[5] M. M. Rashidi, A. Hosseini, I. Pop, S. Kumar, and N. Freidoonimehr, "Comparative numerical study of single and two-phase models of nanofluid heat transfer in wavy channel," *Applied Mathematics and Mechanics*, vol. 35, no. 7, pp. 831–848, May 2014.

[6] M. M. Rashidi, E. Momoniat, M. Ferdows, and A. Basiriparsa, "Lie Group Solution for Free Convective Flow of a Nanofluid Past a Chemically Reacting Horizontal Plate in a Porous Media," *Mathematical Problems in Engineering*, vol. 2014, pp. 1–21, Jan. 2014.

[7] M. Izadi, M. M. Shahmardan, M. J. Maghrebi, and A. Behzadmehr, "Numerical Study Of Developed Laminar Mixed Convection Of Al2o3/Water Nanofluid In An Annulus," *Chemical Engineering Communications*, vol. 200, no. 7, pp. 878–894, Mar. 2013.

[8] M. Izadi, M. M. Shahmardan, and A. Behzadmehr, "Richardson Number Ratio Effect on Laminar Mixed Convection of a Nanofluid Flow in an Annulus," *International Journal for Computational Methods in Engineering Science and Mechanics*, vol. 14, no. 4, pp. 304–316, Jan. 2013.

[9] M. Izadi, A. Behzadmehr, and M. M. Shahmardan, "Effects of discrete source-sink arrangements on mixed convection in a square cavity filled by nanofluid," *Korean Journal of Chemical Engineering*, vol. 31, no. 1, pp. 12–19, Dec. 2013.

[10] N. S. Bondareva, M. A. Sheremet, H. F. Oztop, and N. Abu-Hamdeh, "Heatline visualization of MHD natural convection in an inclined wavy open porous cavity filled with a nanofluid with a local heater," *International Journal of Heat and Mass Transfer*, vol. 99, pp. 872–881, Apr. 2016.

[11] H. Karatas and T. Derbentli, "Natural convection and radiation in rectangular cavities with one active vertical wall," *International Journal of Thermal Sciences*, vol. 123, pp. 129–139, Oct. 2017.

[12] M. M. Charafi, A. Bendaraa, and A. Hasnaoui, "Numerical modelling of natural convection in a square cavity: effect of nanofluid volume fraction and inclination," *MATEC Web of Conferences*, vol. 241, p. 01006, Jan. 2018.

[13] S. Houat and Z. E. Bouayed, "The lattice Boltzmann method for Mixed Convection in a Cavity," *Energy Procedia*, vol. 139, pp. 186–191, Dec. 2017.

[14] Y. Wang, G. Qin, W. He, and Z. Bao, "Chebyshev spectral element method for natural convection in a porous cavity under local thermal non-equilibrium model," *International Journal of Heat and Mass Transfer*, vol. 121, pp. 1055–1072, Mar. 2018.

[15] M. H. Esfe, S. Saedodin, M. Biglari, and H. Rostamian, "Experimental investigation of thermal conductivity of CNTs-Al2O3/water: A statistical approach," *International Communications in Heat and Mass Transfer*, vol. 69, pp. 29–33, Oct. 2015.

[16] K. Khanafer, K. Vafai, and M. Lightstone, "Buoyancy-driven heat transfer enhancement in a two-dimensional enclosure utilizing nanofluids," *International Journal of Heat and Mass Transfer*, vol. 46, no. 19, pp. 3639–3653, May 2003.

[17] M. Kaviany, "Effect of a Protuberance on Thermal Convection in a Square Cavity," *Journal of Heat Transfer*, vol. 106, no. 4, pp. 830–834, Nov. 1984.

[18] N. Freidoonimehr, M. M. Rashidi, and S. Mahmud, "Unsteady MHD free convective flow past a permeable stretching vertical surface in a nano-fluid," *International Journal of Thermal Sciences*, vol. 87, pp. 136–145, Sep. 2014.

[19] R. Mohebbi and M. M. Rashidi, "Numerical simulation of natural convection heat transfer of a nanofluid in an L-shaped enclosure with a heating obstacle," *Journal of the Taiwan Institute of Chemical Engineers*, vol. 72, pp. 70–84, Feb. 2017.

[20] A. A. Mehrizi, M. Farhadi, H. H. Afroozi, K. Sedighi, and A. A. R. Darz, "Mixed convection heat transfer in a ventilated cavity with hot obstacle: Effect of nanofluid and outlet port location," *International Communications in Heat and Mass Transfer*, vol. 39, no. 7, pp. 1000–1008, Apr. 2012.

[21] S. M. Sebdani, M. Mahmoodi, and S. M. Hashemi, "Effect of nanofluid variable properties on mixed convection in a square cavity," *International Journal of Thermal Sciences*, vol. 52, pp. 112–126, Oct. 2011.

[22] R. Mohebbi, M. M. Rashidi, M. Izadi, N. A. C. Sidik, and H. W. Xian, "Forced convection of nanofluids in an extended surfaces channel using lattice Boltzmann method," *International Journal of Heat and Mass Transfer*, vol. 117, pp. 1291–1303, Nov. 2017.

[23] N. C. Markatos and K. A. Pericleous, Laminar and Turbulent Natural Convection in an Enclosed Cavity, Int. J. Heat Mass Transfer. Vol. 27. No. 5, pp. 755-772, 1984

[24] G. de Vahl Davis, Natural convection of air in a square cavity: a benchmark numerical solution, Int. J. Num. Methods Fluids 3, 249-264 (1983).

[25] F. P. Incropera and D. P. DeWitt, Introduction to Heat Transfer, 6th ed. Hoboken, NJ: John Wiley & Sons, 2011.

NOMENCLATURE

S	*Height and Width of Cavity,* M
ϕ	*Fraction of nanoparticle volume,* []
T	*Temperature,* k
x, y	*Dimensional Space Coordinate,* M
g	*Gravitational acceleration,* ms^{-2}
Ra	*Rayleigh number,* []
h	*Heat transfer coefficient,* $W\text{-}m^{-2}K^{-1}$
α	*Thermal diffusivity,* m^2s^{-1}
β	*Thermal expansion coefficient,* K^{-1}
μ	*Dynamic viscosity,* Nsm^{-2}
υ	*Kinematic viscosity,* m^2s^{-1}
ρ	*Density,* kg/m^3
k	*Thermal conductivity,* $W\text{-}m^{-1}K^{-1}$
C_p	*Specific heat,* $J\text{-}kg^{-1}K^{-1}$
Nu	*Nusselt number,* []
nf	*Nanofluid,* []
χ	*x/L Ratio of the enclosure,* []